J. Indian Chem. Soc.,
Vol. 92, December 2015, pp. 1925-1938

Structure, photochromism and mesogenic property of mercury(II) complexes of 1-alkyl-2-(arylazo)imidazoles†

Uttam Panda, Debashis Mallick†, Chandana Sen, Abhijit Nandi, Tapan Kumar Mondal and Chittaranjan Sinha*

Department of Chemistry, Jadavpur University, Kolkata-700 032, India

E-mail : c_r_sinha@yahoo.com

Abstract : $[Hg(Raai\text{-}C_nH_{2n+1})(\mu\text{-}I)I]_2$ (1-alkyl-2-(arylazo)imidazole, Raai-C_nH_{2n+1}, R = H, Me and n = 10, 12, 14, 16, 18, 20, 22) are characterized by spectroscopic data. The structure has been confirmed in case of $[Hg(Haai\text{-}C_{16}H_{33})(\mu\text{-}I)I]_2$ by single crystal X-ray diffraction measurement. Ligands exist at ambient condition in E (*trans*) geometry about azo (-N=N-) group in the chelated motif of the complex. The complexes in DMF solution show E-to-Z (*trans*-to-*cis*) isomerisation of coordinated Raai-C_nH_{2n+1} upon UV light irradiation. The reverse transformation, Z-to-E (*cis*-to-*trans*), is very slow with visible light irradiation and has been carried out by thermal treatment. Quantum yields ($\phi_{E\rightarrow Z}$) of E-to-Z isomerisation are calculated and free ligand shows higher ϕ than their complex phase. The activation energy (E_a) of Z-to-E isomerisation is calculated by controlled temperature experiment (298–308 K). With increasing chain length of -C_nH_{2n+1} in the coordinated ligand the activation energy (E_a) barrier and the activation entropy (ΔS^*) decreases. $[Hg(Meaai\text{-}C_{18}H_{37})(\mu\text{-}I)I]_2$ shows metallomesogenic property and undergoes phase transitions : Cr(50.1°C)–SmA(73.8°C)-I phase sequence on heating and I(131°C)–SmB(71°C)-Cr on cooling. The SmA phase appears as typical Banana shaped on heating cycle while it turns to SmB phase Mosaic texture on cooling.

Keywords : Hg^{II}-arylazoimidazole, X-ray structure, photochromism, metallomesogens, DFT computation.

Introduction

UV light irradiation to azobenzene shows transformation of *trans*-isomer to *cis*-isomer; and reverse, the *cis*-→ *trans*-azobenzene, has been carried out by visible light activation or by thermal excitation. This transformation is defined as 'photochromism'[1–4]. Photoisomerization opens possibilities for a wide range of applications from photoswitches[5], optical data storage devices to molecular machines[6,7]. Azopyridines are effective photochrome because of their chemical interaction with M^{n+} and H^+ [8–10]. Some problems of organic photochrome like photodamage, photodegradation, photochemical reaction could be minimized by binding to metal ions. In search of other azoheterocycles as photochromic motif we have selected series of 1-alkyl-2-(arylazo)imidazoles and have examined their photochromism[11], metal ion coordination[12–17], effect of H^+, and the external factors like solvent (polarity, viscosity, dipole moment etc.), presence of innocent (to be chemically noninteracting) and noninnocent (chemically interacting) ions or molecules[18,19].

Photochromic materials with liquid crystalline properties have large extent of smart applications from data storage to memory devices[20]. However, the synthesis of molecules exhibiting both photochromic and liquid crystalline properties are challenging task. It is due to loss of ordered orientation of liquid crystalline phase upon isomerisation of rod like *trans* (E) to bent *cis* (Z) configuration. We have synthesised long chain 1-alkyl-2-(arylazo)imidazole (Raai-C_nH_{2n+1} where $n > 10$) and some of them exhibit Photochromic Liquid Crystal (PLC) properties[21,22]. In this work, Hg^{II} complexes of Raai-C_nH_{2n+1} (n = 10–22 (even number only)) have been characterised by spectroscopic data (IR, UV-Vis, NMR) and also by single crystal X-ray structure study in one case. Photochromic properties have been examined by optical and thermal relaxation routes. Liquid crystalline properties are examined by polarising

†In honour of Professor Animesh Chakravorty on the occasion of his 80th birth anniversary.

[a]Present address : Mrinalini Datta Mahavidyalaya, Birati, Kolkata-700 051, India.

optical microscopy and differential scanning calorimetry. DFT computation has been attempted to explain the photophysical properties.

Experimental

HgI_2 was prepared by adding KI solution to $Hg(NO_3)_2$ solution, filtered and washed with profuse amount of water. 1-Bromo-n-octane, 1-bromo-n-decane, 1-bromo-n-dodecane, 1-bromo-n-tetradecane, 1-bromo-n-hexadecane, 1-bromo-n-octadecane, 1-bromo-n-icosane, 1-bromo-n-docosane were purchased from Sigma-Aldrich and were of analytical reagent grade and used as received. 1-Alkyl-2-(arylazo)imidazoles were synthesized by reported procedure[20]. All other chemicals and solvents were reagent grade as received and the solvents were purified before use by standard procedures[23].

Physical measurements :

Microanalytical data (C, H, N) were collected on a Perkin-Elmer 2400 CHNS/O elemental analyzer. Spectroscopic data were obtained using the following instruments : UV-Vis spectra from a Perkin-Elmer Lambda 25 spectrophotometer; IR spectra (KBr disk, 4000–200 cm^{-1}) from a Perkin-Elmer RX-1 FTIR spectrophotometer; photoexcitation has been carried out using a Perkin-Elmer LS-55 spectrofluorimeter and ^1H NMR spectra from a Bruker (AC) 300 MHz FTNMR spectrometer. Nikon LV100 POL Corporation Tokyo-8331, Japan and Linkam Heating Stage (THMS 600) Scientific Instruments. Phase transition temperatures were recorded using differential scanning calorimetry (DSC) (Perkin-Elmer Pyris-1 system).

The synthesis of [Hg(Haai-$C_{16}H_{33}$)(μ-I)I]$_2$ (**4a**) :

A solution of HgI_2 (0.20 g, 0.44 mmol) in 2-methoxyethanol (10 ml) was added in drops to a stirred solution of Haai-$C_{16}H_{33}$ (0.19 g, 0.44 mmol) in methanol (10 ml) and the mixture was stirred at dark for 2 h. A dark brown-red precipitate appeared. It was further heated to dissolve and filtered at hot through a G-4 sintered glass crucible. An aqueous solution of KI (0.5 g in 5 ml) was added with constant stirring to this solution to remove any excess of HgI_2. The precipitate so obtained on cooling was collected by filtration, washed with water and recrystallised from 2-methoxyethanol-MeOH (1 : 3, v/v) mixture. It was dried in vacuum and preserved at dark. Yield 0.24 g (65%).

Following identical procedure, other complexes were prepared. Yield 62–72%.

Microanalytical data : Calcd. for $C_{19}H_{28}N_4I_2Hg$ (**1a**), C, 29.76; H, 3.68; N, 7.31. Found : C, 29.95; H, 3.77; N, 7.11%; FT-IR (ν, cm^{-1}) : 1594 (C=N), 1385 (N=N); UV-Vis (λ_{max}/nm, ε × 10^{-3} (M^{-1} cm^{-1})) : 302 (9.1) 365 (17.6), 379 (16.1), 450 (1.4); ^1H NMR (DMSO-d_6) δ, ppm : 7.78 (1H, s, 4-H), 7.30 (1H, s, 5-H), 8.07 (2H, d, *J* 8.5 Hz, 7,11-H), 7.68 (2H, d, *J* 8.3 Hz, 8,10-H), 7.68 (1H, s, 9-H), 4.47 (2H, t, *J* 7.4 Hz, 12-CH_2-), 0.86 (3H, t, *J* 6.1 Hz, 21-CH_3), 1.36–1.24 (16H, bs, 13-20-CH_2-). Calcd. for $C_{20}H_{30}N_4I_2Hg$ (**1b**) : C, 30.76; H, 3.87; N, 7.17. Found : C, 30.64; H, 3.91; N, 7.08%; FT-IR (ν, cm^{-1}) : 1597 (C=N), 1380 (N=N); UV-Vis (λ_{max}/nm, ε × 10^{-3} (M^{-1} cm^{-1})) : 296 (11.4), 368 (18.4), 383 (17.0), 454 (2.1); ^1H NMR (DMSO-d_6) δ, ppm : 7.71 (1H, s, 4-H), 7.32 (1H, s, 5-H), 7.95 (2H, d, *J* 8.7 Hz, 7,11-H), 7.38 (2H, d, *J* 8.3 Hz, 8,10-H), 2.47 (3H, s, 9-CH_3), 4.46 (2H, t, *J* 7.5 Hz, 12-CH_2-), 0.86 (3H, t, *J* 7.0 Hz, 21-CH_3), 1.92–1.24 (16H, bs, 13-20-CH_2-). Calcd. for $C_{21}H_{32}N_4I_2Hg$ (**2a**) : C, 31.73; H, 4.06; N, 7.05. Found : C, 31.65; H, 4.13; N, 7.16%; FT-IR (ν, cm^{-1}) : 1582 (C=N), 1373 (N=N); UV-Vis (λ_{max}/nm, ε × 10^{-3} (M^{-1} cm^{-1})) : 302 (8.1), 365 (11.9), 378 (10.8), 446 (1.2); ^1H NMR (DMSO-d_6) δ, ppm : 7.74 (1H, s, 4-H), 7.29 (1H, s, 5-H), 7.88 (2H, d, *J* 7.8 Hz, 7,11-H), 7.56 (2H, d, *J* 7.9 Hz, 8,10-H), 7.56 (1H, s, 9-H), 4.40 (2H, t, *J* 6.33 Hz, 12-CH_2-), 0.82 (3H, t, *J* 6.1 Hz, 22-CH_3), 1.78–1.14 (20H, bs, 13-21-CH_2-). Calcd. for $C_{22}H_{34}N_4I_2Hg$ (**2b**) : C, 32.66; H, 4.24; N, 6.93. Found : C, 32.50; H, 4.29; N, 6.82%; FT-IR (ν, cm^{-1}) : 1596 (C=N), 1375 (N=N); UV-Vis (λ_{max}/nm, ε × 10^{-3} (M^{-1} cm^{-1})) : 301 (8.2), 368 (17.2), 377 (16.8), 458 (2.2); ^1H NMR (DMSO-d_6) δ, ppm : 7.68 (1H, s, 4-H), 7.28 (1H, s, 5-H), 7.98 (2H, d, *J* 8.0 Hz, 7,11-H), 7.26 (2H, d, *J* 8.1 Hz, 8,10-H), 2.46 (3H, s, 9-CH_3), 4.46 (2H, t, *J* 6.9 Hz, 12-CH_2-), 0.87 (3H, t, *J* 6.3 Hz, 22-CH_3), 1.92–1.24 (20H, bs, 13-21-CH_2-). Calcd. for $C_{23}H_{36}N_4I_2Hg$ (**3a**) : C, 33.57; H, 4.41; N, 6.81. Found : C, 33.67; H, 4.50; N, 6.75%; FT-IR (ν, cm^{-1}) : 1595 (C=N), 1374 (N=N); UV-Vis (λ_{max}/nm, ε × 10^{-3} (M^{-1} cm^{-1})) : 284 (4.8), 367 (16.3), 381 (16.7), 453 (2.0); ^1H NMR (DMSO-d_6) δ, ppm : 7.66 (1H, s, 4-H), 7.24 (1H, s, 5-H), 7.98 (2H, d, *J* 8.2 Hz, 7,11-H), 7.35 (2H, d, *J* 8.2 Hz, 8,10-H), 2.47 (1H, s, 9-H), 4.45 (2H, t, *J* 6.0

Hz, 12-CH_2-), 0.86 (3H, t, *J* 6.1 Hz, 25-CH_3), 1.36–1.25 (24H, bs, 13-24-CH_2-). Calcd. for $C_{24}H_{41}N_{38}I_2Hg$ (**3b**) : C, 34.44; H, 4.58; N, 6.69. Found : C, 34.51; H, 4.62; N, 6.75%; FT-IR (ν, cm^{-1}) : 1593 (C=N), 1376 (N=N); UV-Vis (λ_{max}/nm, ε × 10^{-3} (M^{-1} cm^{-1})) : 292 (15.1), 367 (16.0), 382 (14.1), 456 (1.5); ^{1}H NMR (DMSO-d_6) δ, ppm : 7.78 (1H, s, 4-H), 7.30 (1H, s, 5-H), 8.07 (2H, d, *J* 8.5 Hz, 7,11-H), 7.68 (2H, d, *J* 8.3 Hz, 8,10-H), 7.68 (3H, s, 9-CH_3), 4.47 (2H, t, *J* 7.4 Hz, 12-CH_2-), 0.82 (3H, t, *J* 6.9 Hz, 21-CH_3), 1.79–1.20 (24H, bs, 13-20-CH_2-). Calcd. for $C_{25}H_{40}N_4I_2Hg$ (**4a**) : C, 35.28; H, 4.74; N, 6.58. Found : C, 35.34; H, 4.70; N, 6.64%; FT-IR (ν, cm^{-1}) : 1580 (C=N); 1373 (N=N); UV-Vis (λ_{max}/nm, ε × 10^{-3}(M^{-1} cm^{-1})) : 302 (8.1), 365 (2.5), 380 (27.5), 451 (3.6); ^{1}H NMR (DMSO-d_6) δ, ppm : 7.65 (1H, s, 4-H), 7.25 (1H, s, 5-H), 7.89 (2H, d, *J* 8.2 Hz, 7,11-H), 7.56 (2H, d, *J* 8.3 Hz, 8,10-H), 7.56 (1H, s, 9-H), 4.44 (2H, t, *J* 6.4 Hz, 12-CH_2-), 0.82 (3H, t, *J* 6.0 Hz, 21-CH_3), 1.78–1.20 (28H, bs, 13-20-CH_2-). Calcd. for $C_{26}H_{42}N_4Br_2Pb$ (**4b**) : C, 36.10; H, 4.89; N, 6.48. Found : C, 36.18; H, 4.95; N, 6.43%; FT-IR (ν, cm^{-1}) : 1598 (C=N), 1372 (N=N); UV-Vis (λ_{max}/nm, ε × 10^{-3} (M^{-1} cm^{-1})) : 288 (13.2), 369 (19.1), 382 (16.8), 450 (2.2); ^{1}H NMR (DMSO-d_6) δ, ppm : 7.62 (1H, s, 4-H), 7.21 (1H, s, 5-H), 7.85 (2H, d, *J* 8.1 Hz, 7,11-H), 7.37 (2H, d, *J* 7.7 Hz, 8,10-H), 2.48 (3H, s, 9-CH_3), 4.42 (2H, t, *J* 7.0 Hz, 12-CH_2^-), 0.83 (3H, t, *J* 6.4 Hz, 21-CH_3), 1.39–1.21 (28H, bs, 13-20-CH_2–). Calcd. for $C_{27}H_{44}N_4I_2Hg$ (**5a**) : C, 36.89; H, 5.05; N, 6.37. Found : C, 36.78; H, 5.00; N, 6.22%; FT-IR (ν, cm^{-1}) : 1594 (C=N), 1385 (N=N); UV-Vis (λ_{max}/nm, ε × 10^{-3} (M^{-1} cm^{-1})) : 302 (9.1), 365 (17.6), 379 (16.1), 450 (1.4); ^{1}H NMR (DMSO-d_6) δ, ppm : 7.76 (1H, s, 4-H), 7.24 (1H, s, 5-H), 7.91 (2H, d, *J* 8.3 Hz, 7,11-H), 7.58 (2H, d, *J* 8.4 Hz, 8,10-H), 7.58 (1H, s, 9-H), 4.45 (2H, t, *J* 7.4 Hz, 12-CH_2-), 0.85 (3H, t, *J* 6.1 Hz, 21-CH_3), 1.92–1.23 (32H, bs, 13-20-CH_2-). Calcd. for $C_{28}H_{46}N_4I_2Hg$ (**5b**) : C, 37.66; H, 5.19; N, 6.27. Found : C, 37.72; H, 5.12; N, 6.19%; FT-IR (ν, cm^{-1}) : 1597 (C=N), 1380 (N=N); UV-Vis (λ_{max}/nm, ε × 10^{-3} (M^{-1} cm^{-1})) : 296 (11.4), 368 (18.4), 383 (17.0), 454 (2.1); ^{1}H NMR (DMSO-d_6) δ, ppm : 7.59 (1H, s, 4-H), 7.18 (1H, s, 5-H), 7.93 (2H, d, *J* 8.2 Hz, 7,11-H), 7.29 (2H,d, *J* 8.3 Hz, 8,10-H), 2.46 (3H, s, 9-CH_3), 4.48 (2H, t, *J* 7.5 Hz, 12-CH_2-), 0.85 (3H, t, *J* 7.0 Hz, 21-CH_3), 1.78–1.14 (32H, bs, 13-20-CH_2-). Calcd. for $C_{29}H_{48}N_4I_2Hg$ (**6a**) : C, 38.40; H, 5.33; N, 6.18. Found : C, 38.45; H, 5.38; N, 6.09%; FT-IR (ν, cm^{-1}) : 1582 (C=N), 1373 (N=N); UV-Vis (λ_{max}/nm, ε × 10^{-3} (M^{-1} cm^{-1})) : 302 (8.1), 365 (11.9), 378 (10.8), 446 (1.2); ^{1}H NMR (DMSO-d_6) δ, ppm : 7.76 (1H, s, 4-H), 7.21 (1H, s, 5-H), 7.95 (2H, d, *J* 8.1 Hz, 7,11-H), 7.63 (2H, d, *J* 7.9 Hz, 8,10-H), 7.63 (1H, s, 9-H), 4.38 (2H, t, *J* 6.33 Hz, 12-CH_2-), 0.82 (3H, t, *J* 6.1 Hz, 21-CH_3), 1.93–1.23 (36H, bs, 13-20-CH_2-). Calcd. for $C_{30}H_{50}N_4I_2Hg$ (**6b**) : C, 39.12; H, 5.47; N, 6.08. Found : C, 39.22; H, 5.55; N, 5.92%; FT-IR (ν, cm^{-1}) : 1596 (C=N), 1376 (N=N); UV-Vis (λ_{max}/nm, ε × 10^{-3} (M^{-1} cm^{-1})) : 298 (10.2), 368 (17.2), 377 (16.8), 458 (2.2); ^{1}H NMR (DMSO-d_6) δ, ppm : 7.54 (1H, s, 4-H), 7.16 (1H, s, 5-H), 7.93 (2H, d, *J* 8.3 Hz, 7,11-H), 7.34 (2H, d, *J* 8.1 Hz, 8,10-H), 2.4 (3H, s, 9-CH_3), 4.41 (2H, t, *J* 6.9 Hz, 12-CH_2^-), 0.87 (3H, t, *J* 6.6 Hz, 21-CH_3), 1.79–1.20 (36H, bs, 13-20-CH_2^-). Calcd. for $C_{31}H_{52}N_4I_2Hg$ (**7a**) : C, 39.81; H, 5.60; N, 5.99. Found : C, 39.88; H, 5.66; N, 5.92%; FT-IR (ν, cm^{-1}) : 1594 (C=N), 1375 (N=N); UV-Vis (λ_{max}/nm, ε × 10^{-3} (M^{-1} cm^{-1})) : 284 (4.8), 367 (16.3), 381 (16.7), 453 (2.0); ^{1}H NMR (DMSO-d_6) δ, ppm : 7.52 (1H, s, 4-H), 7.18 (1H, s, 5-H), 7.87 (2H, d, *J* 8.5 Hz, 7,11-H), 7.65 (2H, d, *J* 8.3 Hz, 8,10-H), 7.65 (1H, s, 9-H), 4.44 (2H, t, *J* 7.45 Hz, 12-CH_2-), 0.85 (3H, t, *J* 6.1 Hz, 21-CH_3), 1.66–1.25 (40H, bs, 13-20-CH_2-). Calcd. for $C_{32}H_{54}N_4I_2Hg$ (**7b**) : C, 40.49; H, 5.73; N, 5.90. Found : C, 40.57; H, 5.84; N, 5.83%; FT-IR (ν, cm^{-1}) : 1593 (C=N), 1376 (N=N); UV-Vis (λ_{max}/nm, ε × 10^{-3} (M^{-1} cm^{-1})) : 292 (15.1), 367 (16.0), 382 (14.1), 456 (1.5); ^{1}H NMR (DMSO-d_6) δ, ppm : 7.51 (1H, s, 4-H), 7.14 (1H, s, 5-H), 7.85 (2H, d, *J* 8.2 Hz, 7,11-H), 7.37 (2H, d, *J* 8.3 Hz, 8,10-H), 2.43 (3H, s, 9-CH_3), 4.42 (2H, t, *J* 7.1 Hz, 12-CH_2-), 0.86 (3H, t, *J* 6.9 Hz, 21-CH_3), 1.78–1.20 (40H, bs, 13-20-CH_2).

X-Ray diffraction study :

Suitable single crystal of $[Hg(Haai\text{-}C_{16}H_{33})(\mu\text{-}I)(I)]_2$ (**4a**) (0.22 × 0.26 × 0.33 mm) was mounted on a Siemens CCD diffractometer equipped with graphite monochromated Mo-Kα (λ = 0.71073 Å) radiation. The unit cell parameters and crystal-orientation matrices were determined for two complexes by least squares refinements of all reflections. The intensity data were corrected

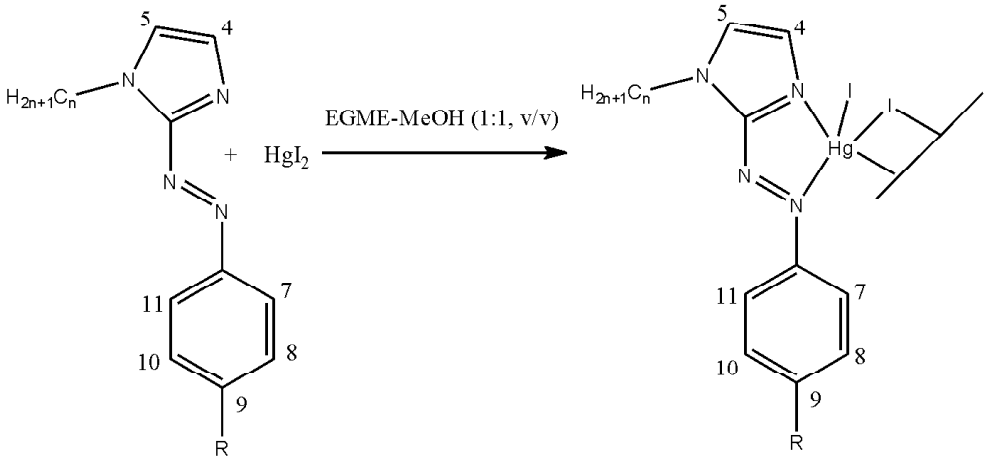

Raai-C_nH_{2n+1} (R = H (**a**), Me (**b**)); [Hg(Raai-C_nH_{2n+1})(μ-I)I]$_2$ (**1-7**)
[Hg(Haai-$C_{10}H_{21}$)(μ-I)I]$_2$ (**1a**), [Hg(Meaai-$C_{10}H_{21}$)(μ-I)I]$_2$ (**1b**), [Hg(Haai-$C_{12}H_{25}$)(μ-I)I]$_2$ (**2a**), [Hg(Meaai-$C_{12}H_{25}$)(μ-I)I]$_2$ (**2b**), [Hg(Haai-$C_{14}H_{29}$)(μ-I)I]$_2$ (**3a**), [Hg(Meaai-$C_{14}H_{29}$)(μ-I)I]$_2$ (**3b**), [Hg(Haai-$C_{16}H_{33}$)(μ-I)I]$_2$ (**4a**), [Hg(Meaai-$C_{16}H_{33}$)(μ-I)I]$_2$ (**4b**), [Hg(Haai-$C_{18}H_{37}$)(μ-I)I]$_2$ (**5a**), [Hg(Haai-$C_{18}H_{37}$)(μ-I)I]$_2$ (**5b**), [Hg(Haai-$C_{20}H_{41}$)(μ-I)I]$_2$ (**6a**), [Hg(Meaai-$C_{20}H_{41}$)(μ-I)I]$_2$ (**6b**), [Hg(Haai-$C_{22}H_{45}$)(μ-I)I]$_2$ (**7a**), [Hg(Haai-$C_{22}H_{45}$)(μ-I)I]$_2$ (**7b**)

Scheme 1. The synthesis of the complexes, [Hg(Raai-C_nH_{2n+1})(μ-I)I]$_2$ (**1-7**).

for Lorentz and polarisation effects and an empirical absorption correction were also employed using the SAINT program[24]. The crystallographic data are shown in Table 1. Data were collected applying the condition $I > 2\sigma(I)$. All these structures were solved by direct methods and followed by successive Fourier and difference Fourier syntheses. Full matrix least squares refinements on F^2 were carried out using SHELXL-97 with anisotropic displacement parameters for all non-hydrogen atoms. Hydrogen atoms were constrained to ride on the respective carbon or nitrogen atoms with an isotropic displacement parameters equal to 1.2 times the equivalent isotropic displacement of their parent atom in all cases. Complex neutral atom scattering factors were used throughout for all cases. All calculations were carried out using SHELXS 97[25], SHELXL97[26], PLATON 99[27].

Table 1. Summarized crystallographic data for [Hg(Haai-$C_{16}H_{33}$)(μ-I)(I)]$_2$ (**4a**)

	[Hg(Haai-$C_{16}H_{33}$)(μ-I)(I)]$_2$
Empirical formula	$C_{50}H_{80}Hg_2I_4N_8$
Formula weight	851
Temperature (K)	296(2)
Crystal system	Triclinic
Space group	P-1
a (Å)	10.2371(3)
b (Å)	10.4828(4)
c (Å)	16.8642(6)
α (°)	105.184(2)
β (°)	95.547(2)
γ (°)	114.031(2)
V (Å)^3	1552.17(9)
Z	2
μ (Mo-Kα) (mm^{-1})	6.965
θ range	2.19–26.45
hkl range	$-12 < h < 12$; $-13 < k < 13$; $-20 < l < 21$
$D_{calcd.}$ (mg m^{-3})	1.821
Refine parameters	231

Table-1 (contd.)

Total reflections	22412
Unique reflections	6308
$R_1{}^a$ [$I > 2\sigma(I)$]	0.0513
$wR_2{}^b$	0.1787
Goodness of fit	1.05

$^aR = \Sigma||F_o| - |F_c||/\Sigma|F_o|$. $^bwR_2 = [\Sigma w(F_o{}^2 - F_c{}^2)^2/\Sigma w(F_o{}^2)^2]^{1/2}$, $w = 1/[\sigma^2(F_o)^2 + (0.1122P)^2 + 1.5755P]$ for **4a**; where $P = (F_o{}^2 + 2Fc^2)/3$.

Photometric measurements :

Absorption spectra were taken with a Perkin-Elmer Lambda 25 UV/Vis spectrophotometer in a 1 × 1 cm quartz optical cell maintained at 25 °C with a Peltier thermostat. The light source of a Perkin-Elmer LS 55 spectrofluorimeter was used as an excitation light, with a slit width of 10 nm. An optical filter was used to cut off

overtones when necessary. The absorption spectra of the *cis* isomers were obtained by extrapolation of the absorption spectra of a *cis*-rich mixture for which the composition is known from ^{1}H NMR integration. Quantum yields (ϕ) were obtained by measuring initial *trans*-to-*cis* isomerization rates (ν) in a well-stirred solution within the above instrument using the equation, $\nu = (\phi I_0/V)(1 - 10^{-Abs})$ where I_0 is the photon flux at the front of the cell, V is the volume of the solution, and Abs is the initial absorbance at the irradiation wavelength. The value of I_0 was obtained by using azobenzene ($\phi = 0.11$ for π-π^* excitation[28]) under the same irradiation conditions.

The thermal E-to-Z (*cis*-to-*trans*) isomerisation rates were obtained by monitoring absorption changes intermittently for a *cis*-rich solution kept in the dark at constant temperatures (T) in the range from 298–308 K. The activation energy (E_a) and the frequency factor (A) were calculated from $\ln k = \ln A - E_a/RT$, where k is the measured rate constant, R is the gas constant, and T is temperature. The values of activation free energy (ΔG^*) and activation entropy (ΔS^*) were obtained through the relationships, $\Delta G^* = E_a - RT - T\Delta S^*$ and $\Delta S^* = [\ln A - 1 - \ln (k_B T/h)/R]$, where k_B and h are Boltzmann's and Plank's constants, respectively.

DFT computation :

The geometry optimization of **4a** was carried out using density functional theory (DFT) at the B3LYP level[29]. All calculations were carried out using the Gaussian 09 program package[30] with the aid of the GaussView visualization program[31]. For C, H, N the 6-31G (d) basis set were assigned, while for Hg and I the LanL2DZ basis set with effective core potential was employed[32,33]. The vibrational frequency calculations were performed to ensure that the optimized geometries represent the local minima and there are only positive eigen values. Vertical electronic excitations based on B3LYP optimized geometries were computed using the time-dependent density functional theory (TD-DFT) formalism in acetonitrile using conductor-like polarizable continuum model (CPCM)[34-36]. Gauss Sum was used to calculate the fractional contributions of various groups to each molecular orbital[37].

Results and discussion

Synthesis and formulation :

The reaction of 1-alkyl-2-(arylazo)imidazole (Raai-C_nH_{2n+1} where R = H (**a**), Me (**b**); n = 10 ($C_{10}H_{21}$, **1**), 12 ($C_{12}H_{25}$, **2**), 14 ($C_{14}H_{29}$, **3**), 16 ($C_{16}H_{33}$, **4**), 18 ($C_{18}H_{37}$, **5**), 20 ($C_{20}H_{41}$, **6**), 22 ($C_{22}H_{45}$, **7**)) with HgI_2 in 2-methoxyethanol-methanol mixture has isolated red-brown complexes $[Hg(Raai\text{-}C_nH_{2n+1})I_2]_2$ (**1-7**). The complexes are purified by diffusion of dichloromethane solution to layered hexane. The composition of the complexes has been supported by microanalytical data. The structural confirmation has been done by single-crystal X-ray diffraction study of one of the complexes. Other spectroscopic techniques (FTIR, UV-Vis, ^{1}H NMR) have been used to characterize the complexes.

The bands in the FT-IR spectra of the complexes (**1-7**) are assigned based on literature report[21,22]. The point of interest is the band due to the azo (-N=N-) and imine (-C=N-) groups in the ligands as well as in the complexes. In free ligands ν(N=N) and ν(C=N) appear at 1400–1410 and 1620–1625 cm^{-1}. The compounds show moderately intense stretching at 1580–1695 and 1370–1385 cm^{-1} are due to ν(C=N) and ν(N=N), respectively. In the complexes, stretching frequency are shifted to lower frequency region which are in support of coordination of azo-N and imine-N to Hg^{II}.

The ^{1}H NMR spectra of the complexes were recorded in DMSO-d_6. The atom numbering pattern is shown in figure (Scheme 1). The alkylation of imidazole is supported by the disappearance of δ(N-H) at ~10.30 ppm and the appearance of N(1)- alkyl signal at 0.85–4.40 ppm; -N-CH_2 -(CH_2)n -CH_3 shows a triplet for -CH_2- at 4.40 ppm, a triplet at 0.85 ppm for -CH_3 group and a multiplet for -(CH_2)n- at 1.22–1.90 ppm. Imidazolyl 4- and 5-H appear as broad singlet at 7.24–7.28 and 7.14–7.17 ppm, respectively (Supplementary Materials, Fig. S1). Broadening may be due to rapid proton exchange between these imidazolic protons. The aryl protons (7-H to 11-H) are upfield shifted on going from phenylazo (**a**) to *p*-tolylazo (**b**) which may be due to +I effect of -Me group. Data (vide Experimental section) reveal that the signals in the spectra of the complexes are shifted to downfield side relative to free ligand values. This supports the coordination of ligand to Hg^{II}. Important feature of the spectra is the shifting of imidazolyl protons 4-H and 5-H to lower δ-values, in general, relative to aryl protons (7-H–11-H). Imidazolyl protons suffer downfield shifting by 0.3–0.4 ppm compared to the free ligand po-

sition. This supports the strong preference of binding of imidazolyl-N to Hg^{II}. Aryl signals shift to the lower field side on Me-substitution to the aryl ring. This is due to electron donating effect of the Me- group.

Molecular structure :

The molecular structure of $[Hg(Haai\text{-}C_{16}H_{33})(\mu\text{-}I)(I)]_2$ (**4a**), is shown in Fig. 1. The bond lengths and angles are listed in Table 2. Each discrete molecular unit consists of dinuclear iodo bridged Hg_2I_2 plane. Haai-$C_{16}H_{33}$ acts as N,N′-chelating ligand (N and N′ refer to N(imidazolyl) and N(azo) donor centres) and a non-bridged-I atom lies in a semi-axial position. The bridged Hg_2I_2 is a parallelogram with two arms Hg(1)-I(1), 2.7077(11) and Hg(1)-I(1)*, 3.2122(9) and the angles are Hg(1)-I(1)-Hg(1a), 88.35(4) and I(1)-Hg(1)-I(1)*, 91.65(3)° (*symmetry : –x,–y,1–z). The atomic arrangements Hg, N(1), C(7), N(3), N(4) constitute chelate plane with a maximum deviation < 0.04 Å and the chelate angle is N(1)-Hg(1)-N(4), 63.46(3)°. Other bond angular values ∠I(1)-Hg-I(2), 128.99(4)°; I(2)-Hg-I(1)*, 100.34(4)°; (*symmetry, –x,–y,1–z) support for distorted geometry. Steric crowding of long chain 1-alkyl group may be the reason for larger deviation[14–16]. The pendant phenyl ring (C(1)-C(6)) makes a small dihedral 8.9° with chelated azoimidazole ring. The Hg-N(imidazolyl) 2.286(9)Å) is shorter than Hg-N(azo) 2.785(2)Å, which reflects stronger interaction between Hg^{II} and N(imidazolyl). The Hg-N distances are longer than previously reported data[14]. Although Hg-N(azo) bond length is long but it is less than the sum of van der Waals radii of Hg^{II} (1.55 Å) and N(sp^2) (1.53 Å). This implies significant bonding interaction between these components. Strong coordination of imidazolyl-N to Hg^{II} has significant biochemical implication and explains strong toxicity of Hg^{II} [38]. Because of long Hg^{II}-N(azo) distance, the molecule may exhibit photophysical activation via cleavage of this bond followed by rotation to introduce photoisomerisation. In fact, we have examined photochromism of these molecules (*vide infra*). The N=N distance is 1.238(11) Å. The Hg-I(bridged) (Hg-I(1), 2.7077(11) Å is longer than Hg-I(non-bridged) (Hg-I(2),

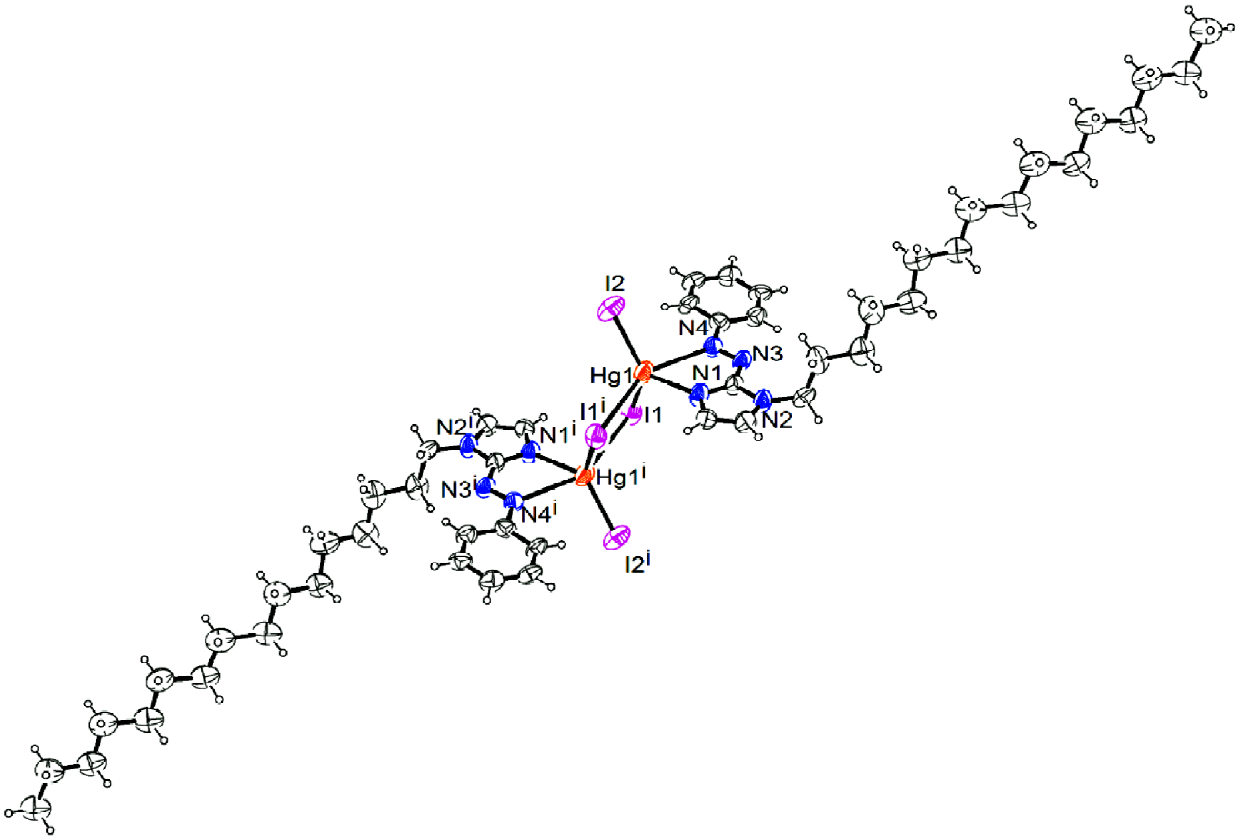

Fig. 1. The molecular structure of $[Hg(Haai\text{-}C_{16}H_{33})(\mu\text{-}I)(I)]_2$ (**4a**).

Table 2. Selected bond distances (Å) and angles (°) for [Hg(Haai-$C_{16}H_{33}$)(μ-I)(I)]$_2$ (**4a**)

Bond distances (Å)		Bond angles (°)	
[Hg(Pai-hexadecane)(μ-I)(I)]$_2$			
Hg(1)-I(1)	2.7077(11)	I(1)-Hg(1)-I(2)	128.99(4)
Hg(1)-I(2)	2.6123(11)	I(1)-Hg(1)-I(1)^a	91.65(3)
Hg(1)-I(1)^a	3.2122(9)	N(1)-Hg(1)-I(2)	120.1(3)
Hg(1)-N(1)	2.286(9)	N(1)-Hg(1)-I(1)	109.7(3)
Hg(1)-N(4)	2.785(2)	N(4)-Hg(1)-I(2)	102.58(9)
N(1)-C(7)	1.349(13)	I(2)-Hg(1)-I(1)^a	100.34(4)
N(2)-C(7)	1.341(13)	Hg(1)-I(1)^a-Hg(1a)	88.35(4)
N(4)-N(3)	1.238(11)	N(1)-Hg(1)-N(4)	63.46(3)
		N(1)–Hg(1)–I(1)	87.7(2)

2.6123(11) Å. The Hg-I(2) is in semi-axial position to their respective plane. Packing view of the crystal structure shows interdigitation of alkyl chain (Fig. 2) which renders supramolecular feature.

380 nm and a tail at 450–465 nm are observed (Supplementary Materials, Fig. S2). The intense transition at shorter wavelength is assigned to π-π* transitions, while the tail is assigned to the admixture of n-π* and MLCT transition from $Hg^{II}\rightarrow\pi^*$(azoimine)[14]. The structural changes are observed in solution phase of coordinated Raai-C_nH_{2n+1} of [Hg(Raai-C_nH_{2n+1})(μ-I)I]$_2$ upon UV light irradiation in DMF solution. The absorption spectrum changes (Fig. 3) in a way similar to that observed for the E-to-Z (*trans*-to-*cis*) isomerization of 1-methyl-2-(arylazo)imidazole[19–21]. The intense peak at λ_{max} decreases along with slight increase at the tail portion of the spectrum around 525 nm until a stationary state is reached. Subsequent irradiation at the newly appeared longer wavelength peak reverses the course of the reaction and the original spectrum is recovered up to a point, which is another photostationary state under irradiation at the longer

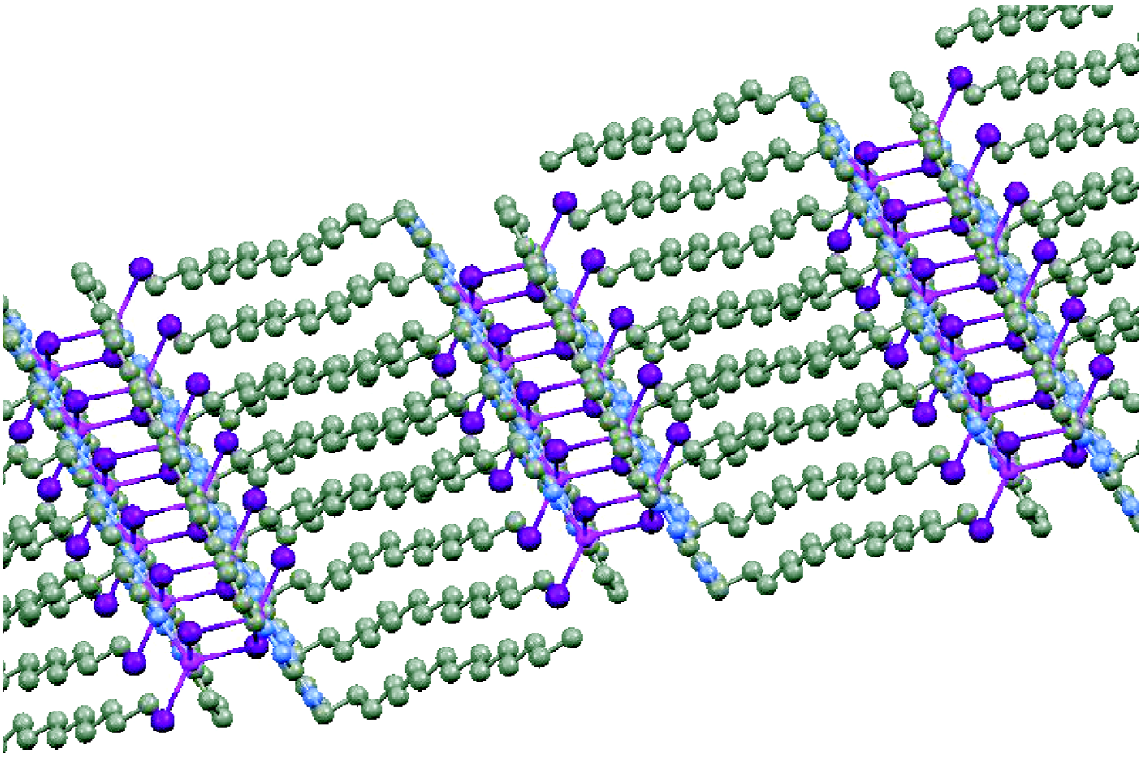

Fig. 2. Interdigitation of long alkyl chain of -$C_{16}H_{33}$ to impose supramolecular network in [Hg(Haai-$C_{16}H_{33}$)(μ-I)I]$_2$.

Photochromism :

The spectra of the complexes are recorded in acetonitrile and the spectral profile is comparable to free ligand characteristics; the structured absorption band around 360–

wavelength peak. The quantum yields of the E-to-Z photoisomerization were determined using those of azobenzene[21,22] as a standard and the results are tabulated in Table 3. The photoisomerisation of ligand in the

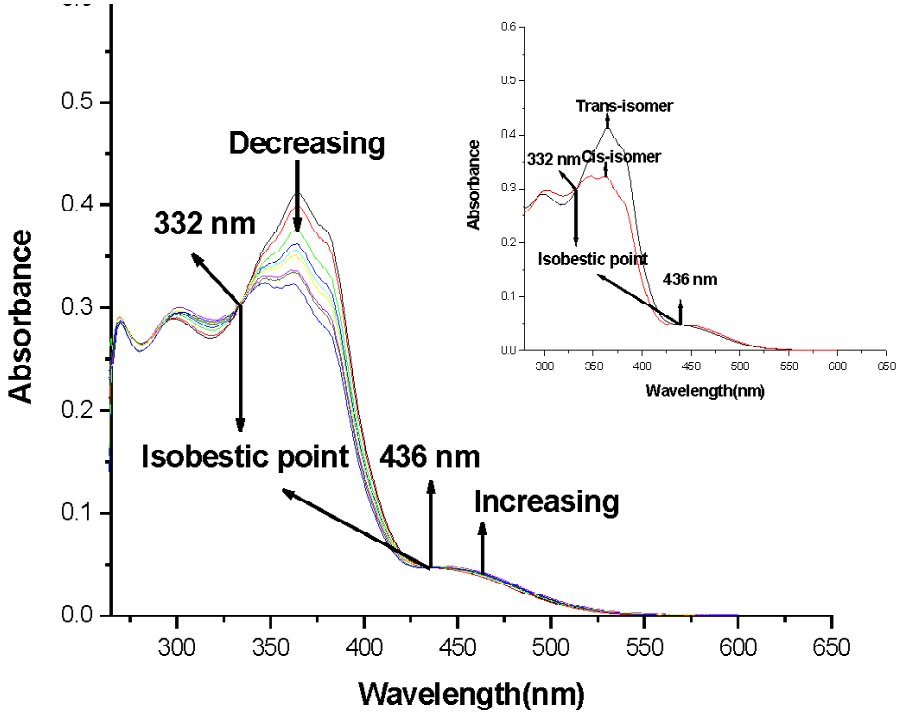

Fig. 3. Spectral changes of $[Hg(Haai\text{-}C_{16}H_{33})(\mu\text{-}I)(I)]_2$ (**4a**) in DMF upon repeated irradiation at 368 nm at 5 min interval at 25 °C. Inset figure shows spectra of Z (*cis*) and *trans* (E) isomer of the complex.

Table 3. Results of photochromism, rate of conversion and quantum yields upon UV light irradiation

Complexes	λ_{π,π^*} (nm)	Isobestic point (nm)	Rate of E→Z conversion × 10^8 (s^{-1})	$\phi_{E\rightarrow Z}$
$[Hg(Haai\text{-}C_{10}H_{21})(\mu\text{-}I)I]_2$ (**1a**)	365	332, 432	1.921	0.106
$[Hg(Meaai\text{-}C_{10}H_{21})(\mu\text{-}I)I]_2$ (**1b**)	367	339, 446	1.837	0.104
$[Hg(Haai\text{-}C_{12}H_{25})(\mu\text{-}I)I]_2$ (**2a**)	368	331, 435	1.834	0.098
$[Hg(Meaai\text{-}C_{12}H_{25})(\mu\text{-}I)I]_2$ (**2b**)	365	334, 442	1.732	0.097
$[Hg(Haai\text{-}C_{14}H_{29})(\mu\text{-}I)I]_2$ (**3a**)	364	335, 435	1.625	0.091
$[Hg(Meaai\text{-}C_{14}H_{29})(\mu\text{-}I)I]_2$ (**3b**)	367	335, 448	1.621	0.090
$[Hg(Haai\text{-}C_{16}H_{33})(\mu\text{-}I)I]_2$ (**4a**)	366	332, 436	1.479	0.085
$[Hg(Meaai\text{-}C_{16}H_{33})(\mu\text{-}I)I]_2$ (**4b**)	369	337, 445	1.325	0.083
$[Hg(Haai\text{-}C_{18}H_{37})(\mu\text{-}I)I]_2$ (**5a**)	367	331, 437	1.321	0.079
$[Hg(Meaai\text{-}C_{18}H_{37})(\mu\text{-}I)I]_2$ (**5b**)	368	331, 446	1.232	0.078
$[Hg(Haai\text{-}C_{20}H_{41})(\mu\text{-}I)I]_2$ (**6a**)	368	336, 436	1.212	0.074
$[Hg(Meaai\text{-}C_{20}H_{41})(\mu\text{-}I)I]_2$ (**6b**)	367	337, 448	1.125	0.073
$[Hg(Haai\text{-}C_{22}H_{45})(\mu\text{-}I)I]_2$ (**7a**)	366	333, 443	1.123	0.071
$[Hg(Meaai\text{-}C_{22}H_{45})(\mu\text{-}I)I]_2$ (**7b**)	368	325, 440	1.119	0.068

complexes are dependent mainly on the molar mass and effective molar volume of photochrome and also on the nature of metal ion, its oxidation state and structure[11–19,21,22]. It is observed that upon irradiation with UV light E-to-Z photoisomerisation proceeded and the Z- (*cis*) molar ratio is reached to ~75%. The absorption spectra of the *trans*-complexes changed with isosbestic points upon excitation into the *cis*-isomer. The ligands and the complexes show little sign of degradation upon repeated irradiation at least upto 15 cycles in each case. The quantum yields were measured for the E-to-Z ($\phi_{E\rightarrow Z}$) photoisomerisation of complexes in DMF on irradiation of UV

wavelength (Table 3). The $\phi_{E\rightarrow Z}$ values are significantly dependent on molar mass and chain length of Raai-C_nH_{2n+1}. The photoisomerisation rate and quantum yield of the complexes re lower than that of free ligand data reported in literature[21].

Thermal Z-to-E (*cis*-to-*trans*) isomerisation of complexes was followed by UV-Vis spectroscopy in DMF at varied temperatures, 298–308 K (Fig. 4). The Eyring plots in the range 298–308 K gave a linear graph from which the activation energy was obtained (Table 4, Fig. 5). In the complexes, the E_as are severely reduced which means faster Z-to-E thermal isomerisation of the complexes. The entropy of activation (ΔS^*) are high negative in the complexes than that of free ligand. This is also in support of increase in rotor volume in the complexes.

The cleavage of Hg-N(azo) bond may cause chelate ring opening followed by rotation about -N=N- bond retaing stronger Hg-N(imidazolyl) bond by UV light irradiation (Scheme 2) may be the plauseable mechanism of photochromism. Sustenance of Hg-N(imidazolyl) bond may be supported from the photostability of these complexes even after prolong irradiation in solution phase. The DFT calculated results of optimized geometry (Supplementary Materials, Tables S1 and S2) of a representative complex, E-isomer [Hg(E-Haai-$C_{16}H_{33}$)(μ-I)(I)]$_2$ (**4a**) and Z-isomer of [Hg(*Z*-Haai-$C_{22}H_{45}$)(μ-I)(I)]$_2$ (**4a′**) have been used to interpret the absorption spectra in gas phase and to explain the photoisomerisation[22]. The optimized struc-

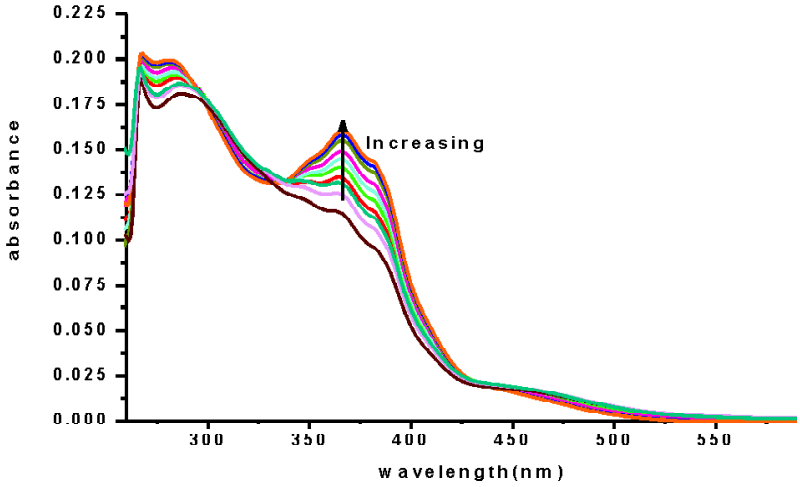

Fig. 4. Z (*cis*) → E (*trans*) spectral changes of [Hg(Haai-$C_{16}H_{33}$)(μ-I)(I)]$_2$ (**4a**) in DMF at 303 K at 5 min interval.

Table 4. Rate and activation parameters for Z (*cis*) → E (*trans*) thermal isomerisation

Complexes	Temp. (K)	Rate of thermal Z→E conversion × 10^3 (s^{-1})	E_a (kJ mol^{-1})	ΔH^* (kJ mol^{-1})	ΔS^* (J mol^{-1} K^{-1})	ΔG^* (kJ mol^{-1})
1a	298	0.3342(3)	56.27(84)	53.75(84)	–131.26(1.17)	93.53(3)
	303	0.4532(3)				
	308	0.6992(2)				
1b	298	0.3443(4)	54.50(54)	51.98(54)	–136.78(1.07)	93.42(2)
	303	0.4953(2)				
	308	0.7032(3)				
2a	298	0.3580(1)	52.66(81)	50.14(81)	–142.64(95)	93.36(3)
	303	0.5035(3)				
	308	0.7139(1)				
2b	298	0.3772(4)	51.81(77)	49.29(76)	–144.95(1.23)	93.21(1)
	303	0.5502(3)				
	308	0.7435(3)				

Table-4 (contd.)

3a	298	0.3903(3)	49.82(32)	47.30(33)	–151.27(1.35)	93.13(1)
	303	0.5803(2)				
	308	0.7492(2)				
3b	298	0.4109(2)	49.10(44)	46.58(43)	–153.24(23)	93.02(2)
	303	0.6035(1)				
	308	0.7815(1)				
4a	298	0.4235(3)	48.54(55)	46.02(55)	–154.89(1.07)	92.95(3)
	303	0.6203(3)				
	308	0.7995(3)				
4b	298	0.4409(4)	46.74(37)	44.22(36)	–160.59(1.01)	92.87(3)
	303	0.6408(1)				
	308	0.8129(1)				
5a	298	0.4532(2)	46.58(81)	44.07(81)	–160.86(11)	92.80(1)
	303	0.6593(2)				
	308	0.8339(1)				
5b	298	0.4609(2)	45.90(69)	43.39(70)	–163.00(1.12)	92.77(2)
	303	0.6778(3)				
	308	0.8403(2)				
6a	298	0.4732(1)	44.82(45)	42.30(45)	–166.31(34)	92.69(3)
	303	0.7132(3)				
	308	0.8530(3)				
6b	298	0.4805(2)	44.52(56)	42.00(56)	–167.14(57)	92.69(3)
	303	0.7339(2)				
	308	0.8599(3)				
7a	298	0.4992(4)	41.92(44)	39.40(44)	–175.48(1.07)	92.57(2)
	303	0.7683(4)				
	308	0.8632(1)				
7b	298	0.5232(2)	41.89(57)	39.38(57)	–175.30(13)	92.49(1)
	303	0.7676(3)				
	308	0.9049(3)				

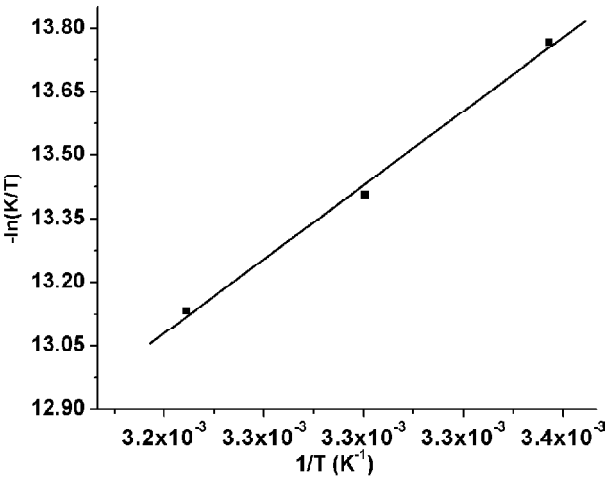

Fig. 5. The Eyring plot of rate constants of Z-to-E thermal isomerisation of [Hg(Haai-$C_{16}H_{33}$)(μ-I)(I)]$_2$ (**4a**) at different temperatures.

ture of E-isomer is more stable than Z-isomer by 205 kcal mol^{-1} (8.9 eV) (Fig. 6). The HOMO (highest occupied molecular orbital) (–5.81 eV), HOMO-1 (–6.23 eV); HOMO-2 (–6.42 eV), HOMO-3 (–6.56 eV); HOMO-4 (–6.86 eV), HOMO-5 (–6.97 eV) and the LUMO (lowest unoccupied molecular orbital) (–3.56 eV), LUMO+1 (–3.32 eV), LUMO+2 (–0.89 eV), LUMO+3 (–0.71 eV), LUMO+4 (–0.31 eV), LUMO+5 (–0.26 eV) show varying degree of composition and energy. The MOs of Z-isomer are also distributed as follows : HOMO (–5.46 eV), HOMO-1 (–6.04 eV), HOMO-2 (–6.24 eV), LUMO (–3.81 eV), LUMO+1 (–3.39 eV), LUMO+2 (–0.93 eV) etc. The HOMO is stabilized by 0.35 eV (8.05 kcal) in E-isomer while LUMO is stabilized by 0.25 eV (5.75 kcal) in Z-isomer. High intense bands calculated at 452

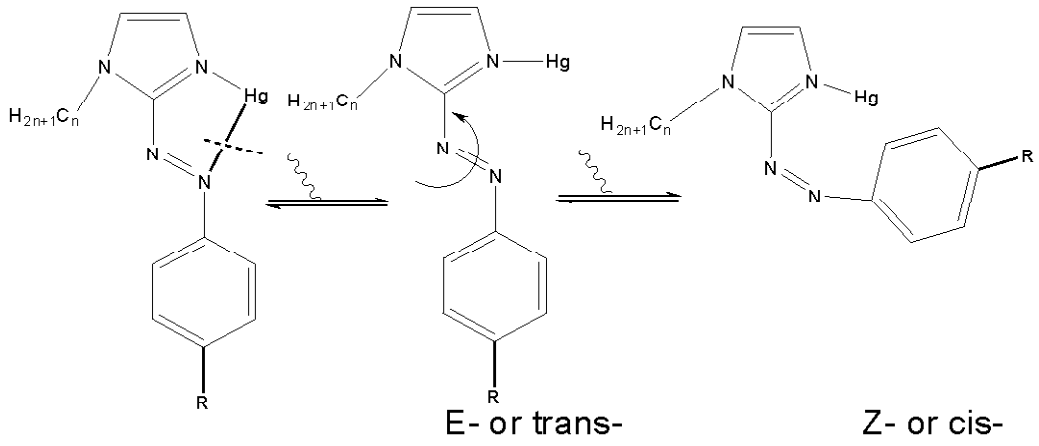

Scheme 2. Plausible mechanism of photoisomerisation of coordinated Raai-C_nH_{2n+1} in [Hg(Raai-C_nH_{2n+1})] motif in the complex.

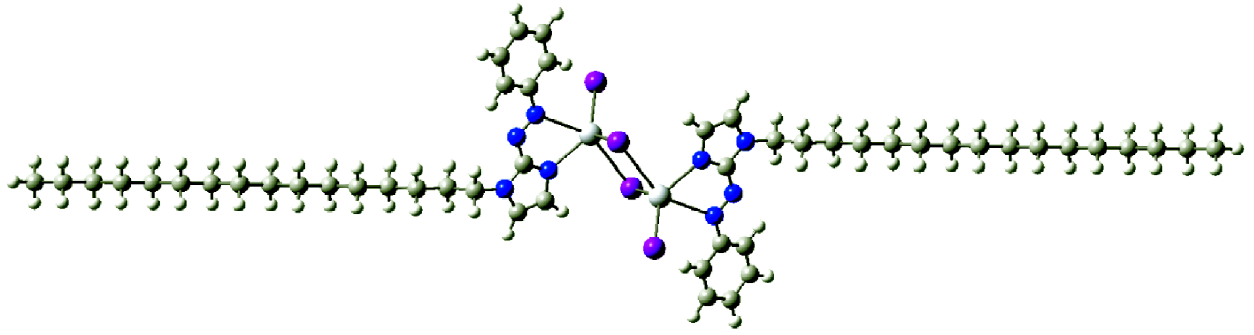

E-[[Hg(Haai-$C_{16}H_{33}$)(μ-I)I]$_2$] , E = –68635.37 eV mol^{-1} (**4a**)

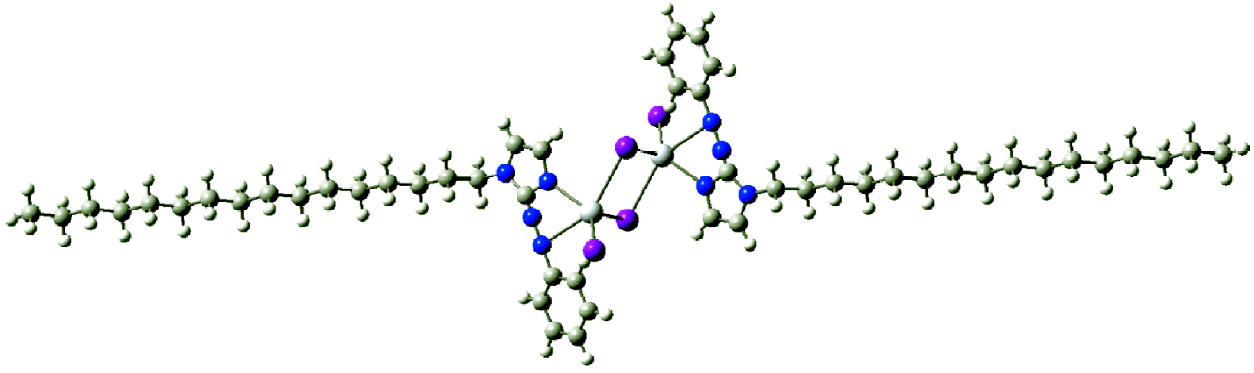

Z-[[Hg(Haai-$C_{16}H_{33}$)(μ-I)I]$_2$] , E = –68626.47 eV mol^{-1} (**4a′**)

Fig. 6. Optimized structures of E- and Z-[Hg(Haai-$C_{16}H_{33}$)(μ-I)I]$_2$ (**4a** and **4a′**).

nm (oscillator strength *f*, 0.1176), 381 nm (*f*, 0.1386), 365 nm (*f*, 0.3279) are referred to HOMO-2 LUMO → HOMO-6 → LUMO+2, HOMO-1 → LUMO+3 transitions, respectively those have been assigned mainly to halide(X)-to-ligand charge transfer (XLCT) band (Supplementary Materials, Tables S3, Fig. S3). The energy separation between HOMO-LUMO (ΔE = 1.65 eV or 37.95 kcal mol^{-1}) also indicates the generation of low energy band (~450 nm) upon UV light irradiation which indicates the population increment of Z-isomer.

Upon UV light irradiation the stable *trans*-derivative

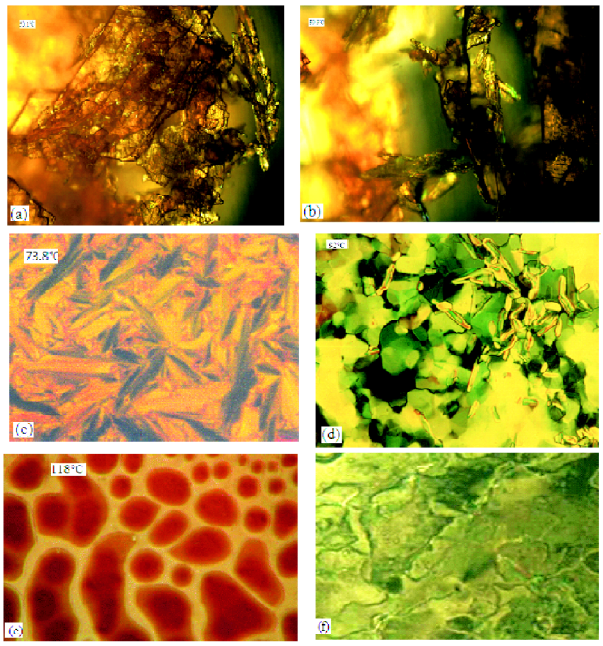

Fig. 7. POM views of different phases at respective temperature (noted in the photograph) at heating phase (a) at 50.1 °C (crystalline), (b) 59.3 °C (melting start), (c) 73.8°C (SmA) and (d) 92 °C (banana shape) and (e) isotropic phase at 118 °C of $[Hg(Meaai\text{-}C_{16}H_{33})I_2]_2$ and (f) on cooling phase (71 °C) mosaic texture.

(E) isomerizes to *cis*-derivative (Z). Irradiation in the UV region causes $\pi \rightarrow \pi^*$ transition which is responsible for cleavage of Hg-N(azo) bond and opening of chelate ring followed by E→Z geometry change. The LMCT (ligand-to-metal charge transition) or CRCT (chain-to-ring charge transition) are of lower energetic transition and is insufficient to perform bond cleavage and isomerisation.

Metallomesogenic properties :

The thermal properties of the complexes have been examined using polarized light optical microscopy (POM) and differential scanning calorimetry (DSC). Some of the ligands with long alkyl chain, Raa-C_nH_{2n+1} are active under POM during thermal treatment[21,22]; Haai-$C_{18}H_{37}$ shows nematic (N) texture at 55 °C and on cooling isotropic phase of Haai-$C_{18}H_{37}$ transforms to 'Schlieren' phase. Haai-$C_{22}H_{45}$ shows unknown Smectic (Sm) phase at 62 °C. The textural analysis of $[Ag(Raai\text{-}C_nH_{2n+1})_2]ClO_4$ shows that only $[Ag(Haai\text{-}C_{18}H_{37})_2]ClO_4$ is active to the phase[22] sequence Cr-SmC (fan shaped)-I phases on heating and on cooling the sequence follows I-SmA-Cr. Out of fourteen complexes only $[Hg(Meaai\text{-}C_{16}H_{33})(\mu\text{-}I)I]_2$ (**4b**) shows mesomorphic activity. Upon melting, the crystalline solid turns to jelly type materials, which displays various types of smetic phases. The complex starts to melt around 50 °C indicated by a cloudy appearance and the process completed around 128 °C. During this process, at first focal conic fan textures were found from 50.1 °C to 71 °C (Fig. 7). Finally at 73.8 °C SmA phase mesogene is observed. The SmA phase turns to banana shaped on heating cycle at 92 °C and on fur-

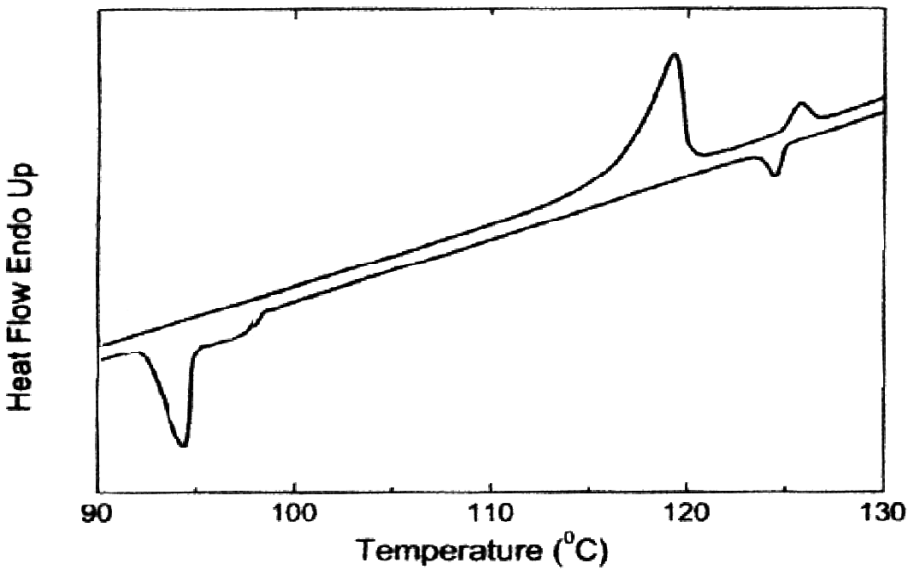

Fig. 8. The DSC of $[Hg(Haai\text{-}C_{16}H_{33})(\mu\text{-}I)I]_2$ (**4a**) at the rate of 2 °C min^{-1} (94 °C (exo), 118.9 °C (endo), 125 °C (exo), 122 °C (endo)).

ther heating isotropic phase appears at 118 °C. The cooling cycles is very complex and proceed through large number of phases those are difficult to distinguish; however at 71 °C SmB phase Mosaic texture is observed. The differential scanning calorimetry (DSC) (Fig. 9) of this complex shows ΔH (26.4 J/g) at 94 °C and endothermic response at 118.9 °C (32.1 J/g). A small peak arises at 122 °C, where ΔH is very low (1.68 J/g) indicates a transition from crystal to Mosaic texture of smectic B textures.

Conclusion

Hg^{II}-iodo-bridging dimer of chelated 1-alkyl-2-(arylazo)imidazoles, $[Hg(Raai\text{-}C_nH_{2n+1})(\mu\text{-}I)I]_2$ are characterized by spectroscopic techniques and single crystal X-ray structure of one of the complexes the geometry of the complex. Raai-C_nH_{2n+1} shows E-(*trans*)–Z(*cis*) isomerisation upon UV-light irradiation both in free and coordinated state. Rate and quantum yields of the isomerisation are largely dependent on the rotor mass of the photochromes. The Z-to-E isomerisation is thermally driven process. The activation energy (E_as) and ΔS^* are decreasing with increasing mass and chain length of alkyl group, -C_nH_{2n+1}. One of the complexes, $[Hg(Meaai\text{-}C_{16}H_{33})(\mu\text{-}I)I]_2$ shows metallomesogenic property and undergoes phase transitions : Cr(50.1 °C)-SmA(73.8 °C)-I phase sequence on heating and I(131 °C)-SmB (71 °C)-Cr on cooling. The SmA phase appears as typical Banana shaped on heating cycle while it turns to SmB phase Mosaic texture on cooling.

Supplementary material

Crystallographic data for the structures have been deposited with the Cambridge Crystallographic Data Center; CCDC No. 1434102. Copies of this information may be obtained free of charge from the Director, CCDC, 12 Union Road, Cambridge CB2 1EZ, UK (E-mail, deposit@ccdc.cam.ac.uk,or www,htpp:// www.ccdc.cam.ac.uk).

Acknowledgement

The authors express their sincere thanks to Department of Science and Technology (DST), West Bengal Government (228/1(10)/(Sanc.)/ST/P/S&T/9G-16/2012), Kolkata and the Council of Scientific and Industrial Research (01(2731)/13/EMR-II), New Delhi for financial support. DM acknowledges UGC Minor Research Project (F.PSW-158/13-14) for financial support.

References

1. G. H. Brown (Ed.), "Photochromism", Wiley-Intersciences, New York, 1971.
2. H. Rau, in "Photochromism : Molecules and Systems", eds. H. Dürr and H. Bouas-Laurent, Elsevier, Amsterdam, 1990.
3. R. Guglielmetti, "Photochromism : Molecules and Systems", eds. H. Dürr and H. Bouas-Laurent, Elsevier, Amsterdam, 1990, pp. 314-466 and 855-878.
4. R. C. Bertelson, "Organic Photochromic and Thermochromic Compounds", eds. J. C. Crano, R. Guglielmetti, Plenum Press, New York, 1999, pp. 11-83.
5. B. L. Feringa (Ed.), "Molecular Switches", Wiley-VCH, Weinheim, 2001.
6. R. Tel-Vered and I. Willner, "Designing Receptors for the Next Generation of Biosensors", 'Springer Series on Chemical Sensors and Biosensors', eds. S. A. Piletsky and M. Whitcombe, Springer-Verlag, Berlin Heidelberg, 2013, pp. 189-212.
7. G. Pace, V. Ferri, C. Grave, M. Elbing, C. von Hänisch, M. Zharnikov, M. Mayor, M. A. Rampi and P. Samorì, *Proc. Natl. Acad. Sci. (USA)*, 2007, **104**, 9937.
8. T. Michinobu, R. Eto, H. Kumazawa, N. Fujii and K. Shigehara, *J. Macromol. Sci., Part A*, 2011, **48**, 625.
9. K. Suwa, J. Otsuki and K. Goto, *J. Phys. Chem. (A),* 2010, **114**, 884.
10. S. Kume and H. Nishihara, *Dalton Trans.,* 2008, 3260.
11. J. Otsuki, K. Suwa, K. Narutaki, C. Sinha, I. Yoshikawa and K. Araki, *J. Phys. Chem. (A),* 2005, **109**, 8064; J. Otsuki, K. Suwa, K. K. Sarker and C. Sinha, *J. Phys. Chem. (A),* 2007, **111**, 1403.
12. K. K. Sarker, D. Sardar, K. Suwa, J. Otsuki and C. Sinha, *Inorg. Chem.,* 2007, **46**, 8291.
13. K. K. Sarker, A. D. Jana, G. Mostafa, J.-S. Wu, T.-H. Lu and C. Sinha *Inorg. Chim Acta,* 2006, **359**, 4377.
14. D. Mallick, A. Nandi, S. Datta, K. K. Sarker, T. K. Mondal and C. Sinha, *Polyhedron*, 2012, **31**, 506; S. Saha (Halder), P. Raghavaiah and C. Sinha, *Polyhedron*, 2012, **46**, 25.
15. D. Mallick, K. K. Sarker, P. Datta, T. K. Mondal and C. Sinha, *Inorg. Chim. Acta,* 2012, **387**, 352.
16. S. Saha (Halder), B. G. Chand, J.-S. Wu, T.-H. Lu, P. Raghavaiah and C. Sinha, *Polyhedron*, 2012, **46**, 81; C. Sen, A. Nandi, D. Mallick, S. Mondal, K. K. Sarker and C. Sinha, *Spectrochim. Acta (A)*, 2015, **137**, 935.
17. D. Das, J. Dinda, T. Mondal, K. K. Sarker and C. Sinha, *J. Indian Chem. Soc.,* 2006, **83**, 861; S. Saha (Halder), P. Mitra and C. Sinha, *Polyhedron*, 2014,

67, 321; P. Datta, D. Mallick, T. K. Mondal and C. Sinha, *Polyhedron*, 2014, **71**, 47; P. Dutta, D. Mallick, S. Roy, E. L. Torres and C. Sinha, *Inorg. Chim. Acta,* 2014, **423**, 397; C. Sen, D. Mallick, S. Mondal and C. Sinha, *J. Indian Chem. Soc.,* 2015, **92**, 203.

18. P. Gayen and C. Sinha, *J. Lumin.,* 2012, **132**, 2371; P. Gayen and C. Sinha, *Spectrochim. Acta, Part A,* 2012, **98**, 116; P. Gayen, K. K. Sarker and C. Sinha, *Colloids and Surfaces (A)*, 2013, **429**, 60.
19. P. Gayen and C. Sinha, *Spectrochim. Acta, Part A,* 2013, **104**, 477; P. Gayen and C. Sinha, *J. Indian Chem. Soc.*, 2013, **90**, 751; P. Gayen, T. K. Misra and C. Sinha, *J. Spectrosc. Dyn.*, 2014, **4**, 27.
20. I. Muševiè and S. Žumer, *Nature Mate.,* 2011, **10**, 266.
21. A. Nandi, C. Sen, D. Mallick, R. K. Sinha and C. Sinha, *Adv. Mater. Phys. Chem.,* 2013, **3**, 133.
22. A. Nandi, C. Sen, S. Roy, D. Mallick, R. K. Sinha, T. K. Mondal and C. Sinha, *Polyhedron*, 2014, **79**, 186.
23. A. I. Vogel, "A Text Book of Practical Organic Chemistry", 2nd ed., Longman, London 1959.
24. G. M. Sheldrick, SHELXS 97, Program for the Solution of Crystal Structure, University of Gottingen, Germany, 1997.
25. G. M. Sheldrick, SHELXL 97, Program for the Solution of Crystal Structure, University of Gottingen, Germany, 1997.
26. A. L. Spek, PLATON, Molecular Geometry Program, University of Utrecht, The Netherlands, 1999.
27. L. J. Farrugia, ORTEP-3 for window, *J. Appl. Cryst.,* 1997, **30**, 565.
28. G. Zimmerman, L. Chow and U. Paik, *J. Am. Chem. Soc.,* 1958, **80**, 3528.
29. P. J. Hay and W. R. J. Wadt, *J. Chem. Phys.,* 1985, **82**, 299.
30. M. J. Frisch, G. W. Trucks, H. B. Schlegel, G. E. Scuseria, M. A. Robb, J. R. Cheeseman, G. Scalmani, V. Barone, B. Mennucci, G. A. Petersson, H. Nakatsuji, M. Caricato, X. Li, H. P. Hratchian, A. F. Izmaylov, J. Bloino, G. Zheng, J. L. Sonnenberg, M. Hada, M. Ehara, K. Toyota, R. Fukuda, J. Hasegawa, M. Ishida, T. Nakajima, Y. Honda, O. Kitao, H. Nakai, T. Vreven, J. A. Montgomery (Jr.), J.E. Peralta, F. Ogliaro, M. Bearpark, J. J. Heyd, E. Brothers, K. N. Kudin, V. N. Staroverov, R. Kobayashi, J. Normand, K. Raghavachari, A. Rendell, J. C. Burant, S. S. Iyengar, J. Tomasi, M. Cossi, N. Rega, J. M. Millam, M. Klene, J. E. Knox, J. B. Cross, V. Bakken, C. Adamo, J. Jaramillo, R. Gomperts, R. E. Stratmann, O. Yazyev, A. J. Austin, R. Cammi, C. Pomelli, J. W. Ochterski, R. L. Martin, K. Morokuma, V. G. Zakrzewski, G. A. Voth, P. Salvador, J. J. Dannenberg, S. Dapprich, A. D. Daniels, Ö. Farkas, J. B. Foresman, J. V. Ortiz, J. Cioslowski, D. J. Fox, GAUSSIAN 09, Revision D.01, Gaussian Inc.,Wallingford, CT, 2009.
31. A. Frisch, A. B. Nielson and A. J. Holder, GAUSSVIEW User Manual, Gaussian Inc, Pittsburgh, PA, 2000.
32. P. J. Hay and W. R. Wadt, *J. Chem. Phys.*, 1985, **82**, 270.
33. W. R. Wadt and P. J. Hay, *J. Chem. Phys.,* 1985, **284**, 284.
34. M. E. Casida, C. Jamorski, K. C. Casida and D. R. Salahub, *J. Chem. Phys.,* 1998, **108**, 4439.
35. V. Barone and M. Cossi, *J. Phys. Chem. (A),* 1998, **102**, 1995.
36. M. Cossi and V. Barone, *J. Chem. Phys.*, 2001, **115**, 4708.
37. M. Cossi, N. Rega, G. Scalmani and V. Barone, *J. Comput. Chem.*, 2003, **24**, 669.
38. J. E. Fergusson, "The Heavy Elements : Chemistry, Environment Impact and Health Effects", Pergamon, Oxford, 1990.